

Is Your AAV Payload Impacting Stability?

Find out with Aura GT

Introduction

Adeno-associated viruses (AAVs) have transformed gene therapies by enabling the targeted delivery of therapeutic genetic payloads. However, the amount of AAV material available is consistently in short supply due to its inherently expensive, time-consuming, and laborious production process.¹ This hampers early-stage physical stability characterization, particularly subvisible particle (SVP) analysis which is a critical quality attribute. The presence of SVPs in a biotherapeutic can lead to adverse immune reactions and reductions in therapeutic efficacy.² The composite DNA/protein nature of AAVs presents an analytical challenge when determining the root causes of subvisible particle formation. AAV capsids are meta-stable: the protein shell must be strong enough to withstand the drug delivery journey, but rupture once inside the cell to release the therapeutic payload.³ Compromised AAV capsid integrity can potentially lower product purity and significantly reduce drug efficacy. It is also well established that DNA can promote aggregate formation,⁴ a behavior that may be enhanced when DNA leaks out of the AAV protein capsid. Understanding how capsid proteins interact with leaked DNA payloads is essential to avoid AAV aggregation and ensure high quality drug product development, control, and shelf-life. However, deciphering the role of DNA in the formation of subvisible particles in AAV formulations has been difficult if not impossible to determine until this point, hampered by legacy systems

that cannot conduct low volume subvisible particle analysis or interrogate for DNA content.

This application note demonstrates how [Halo Labs' Aura GT™](#), powered by [Fluorescence Membrane Microscopy \(FMM\)](#), helps monitor nucleic acid leakage that can occur under common storage conditions, increasing subvisible particle formation in an industrially relevant gene therapy sample. Empty and full capsid controls were used in this study. High-throughput subvisible imaging, counting, sizing, and identification was conducted using Brightfield (BF) [backgrounded membrane imaging \(BMI\)](#) and FMM with SYBR™ Gold Nucleic Acid Stain.

Method

Full and Empty AAV Capsid Production: Purified AAV was separated into empty and full capsid populations, both with >95% purity. Both empty and full capsids were stressed at 30 °C for one week.

Aura GT: Aura GT was used to perform BMI and FMM particle imaging, sizing, and counting. FMM can be used to detect free DNA by exciting SYBR Gold (Thermo Fisher catalog no. S11494) fluorescence at 488 nm and measuring the emission at 550 nm. The respective samples were applied to an Aura black membrane plate (40 µL per well) and stained with SYBR Gold at 10x staining concentration for 5 minutes. Wells were then imaged in both BMI and the SYBR Gold fluorescence channel.

DNA and Protein Controls: 2 μm amine conjugated DNA binding beads (Millipore-Sigma, catalog no. L0280) were used in the presence and absence of DNA as positive controls. In addition, empty wells (not shown) and thermally stressed bovine serum albumin (BSA) (Millipore-Sigma, catalog no. SRE0096) were used as additional non-specific interaction controls.

Results

Aura GT FMM Detects SYBR Gold Labeled DNA

The ability of SYBR Gold to stain DNA on samples filtered on the membrane plates was first evaluated using Aura GT via 2 μm amine labeled beads in the presence and absence

of DNA (Figure 1). The DNA-bound beads displayed significantly higher SYBR Gold staining (Figure 1a, 1c) than the unlabeled beads (Figure 1b, 1d), which displayed almost zero fluorescent signal in the SYBR Gold channel. Additionally, the presence of DNA on the bead surface enhanced aggregation of the colloid beads when compared to the beads without DNA. Scatter plots of SYBR Gold fluorescence intensity vs. particle size (equivalent circular diameter, μm) shown in Figure 2 confirm that the labeled beads exhibited much more particle aggregation (most particles detected were larger than 2 μm bead singlet size) and stronger fluorescence, while the unlabeled beads produced few subvisible particles and were virtually unstained by SYBR Gold.

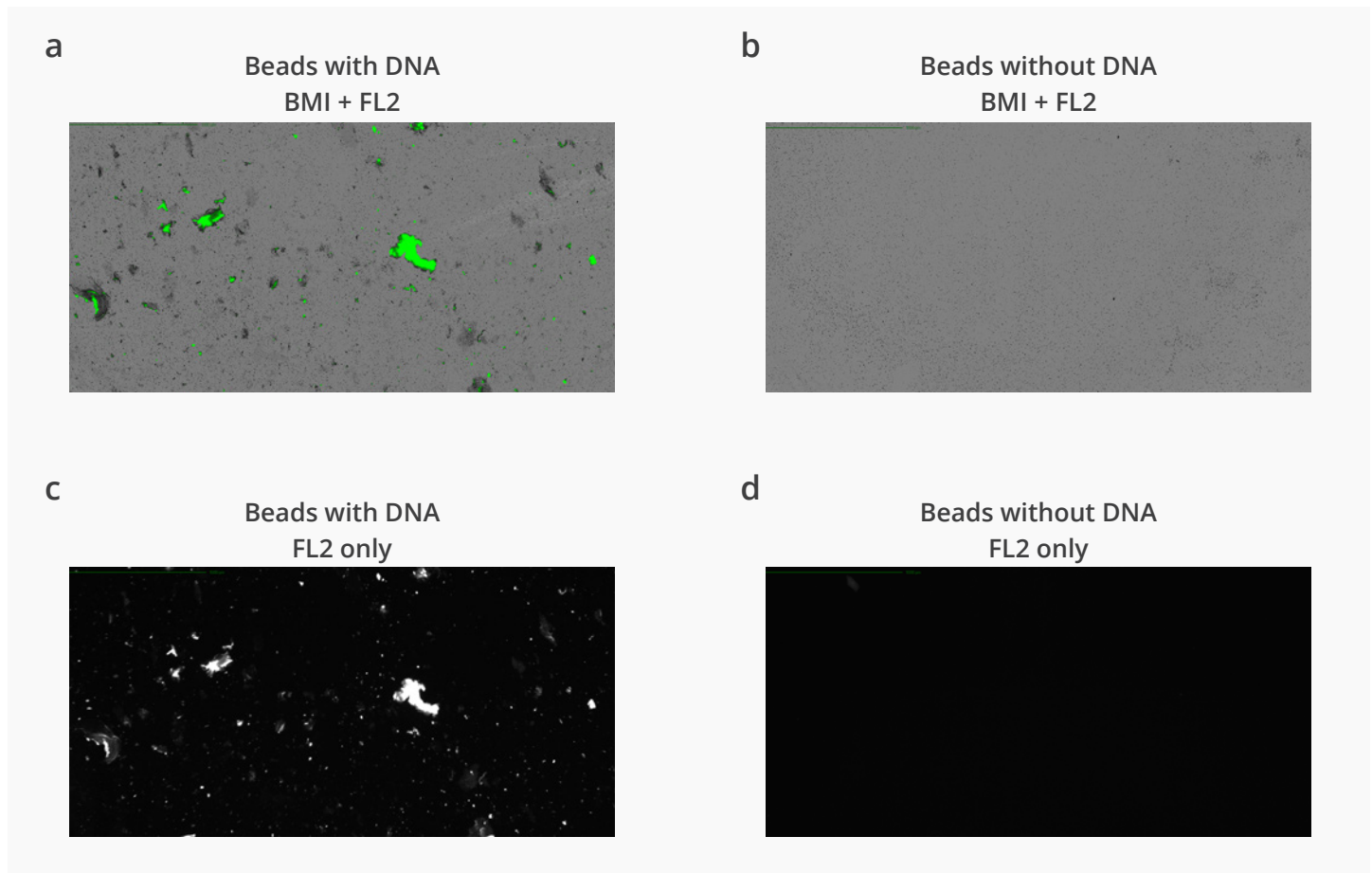


Figure 1: Specific detection of SYBR labeled colloid beads using Aura GT. (a, c) DNA coated colloid beads and (b, d) beads without DNA were analyzed. (a, b) Beads were imaged with combined Brightfield + SYBR Gold (green) fluorescence and (c, d) SYBR Gold fluorescence only.

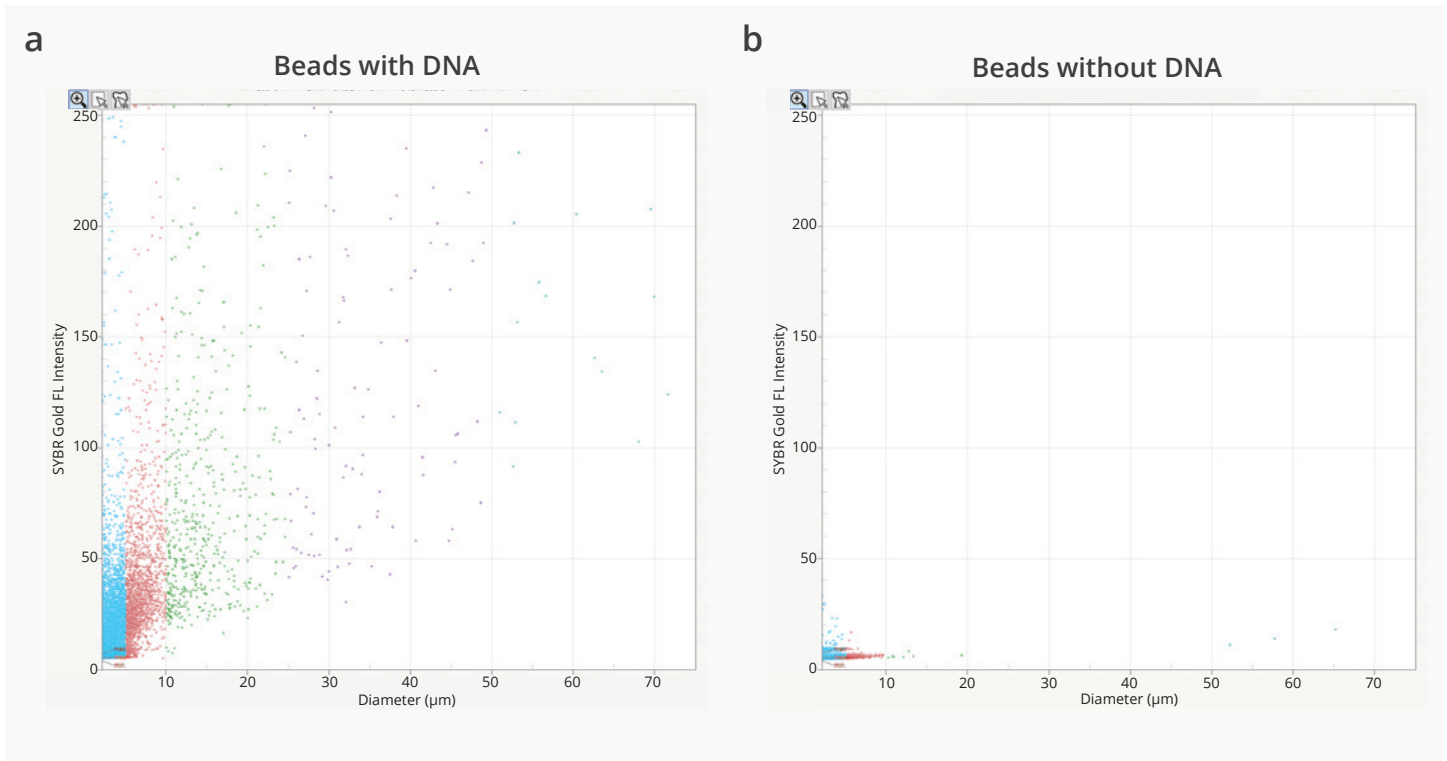


Figure 2: Scatter plot data for (a) DNA labeled colloid beads and (b) beads without DNA. The y-axis represents fluorescence intensity in the SYBR Gold channel, the x-axis represents the equivalent circular diameter (ECD) in μm. Each point represents the average fluorescence intensity for an individual subvisible particle. Beads linked with DNA exhibited much higher particle aggregation and SYBR Gold fluorescence.

As an additional specificity control, we used BSA (50 μg/mL) to confirm that the SYBR Gold does not stain protein aggregates and was selective only to DNA as shown in Figure 3. Figure 3a shows that the presence

of significant subvisible BSA protein aggregates, while Figure 3b shows that these did not fluoresce under SYBR Gold fluorescence.

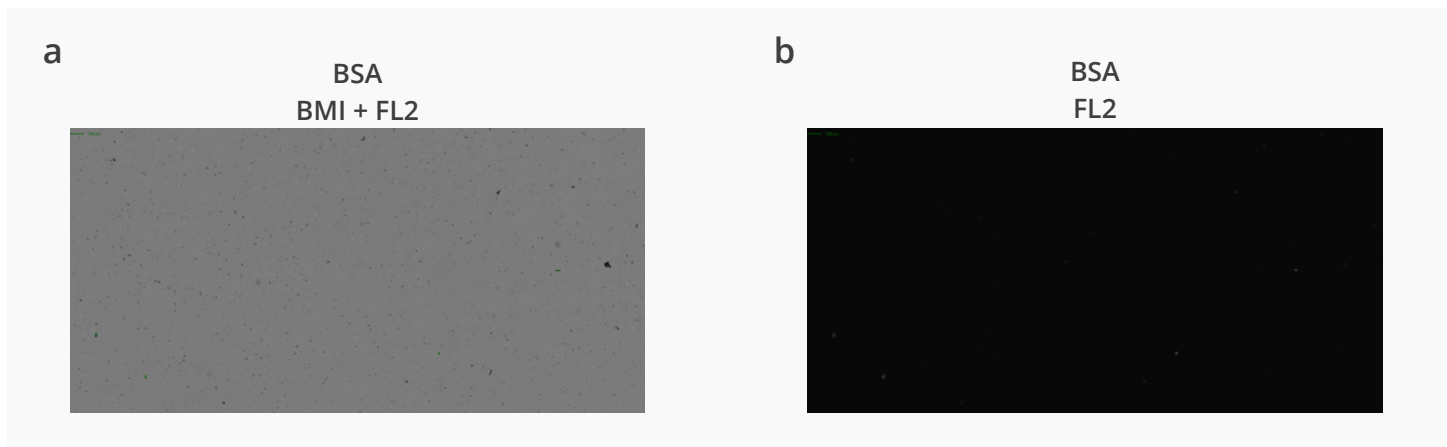


Figure 3: DNA labeling with SYBR Gold is specific. Aggregated BSA was stained with SYBR Gold to determine the level of non-specific protein staining. Specificity was confirmed when no virtually no SYBR fluorescence signal from non-specific adsorption into proteins was observed.

Quantifying Subvisible Particle Aggregation and DNA Leakage in Full and Empty AAV Samples

SYBR Gold was applied to both full and empty AAV capsids fractions from a commercial partner to determine whether the AAV capsid itself was sensitive to SYBR Gold staining and whether SYBR Gold fluorescence is a suitable probe to detect DNA in subvisible AAV aggregates. The images in Figure 4 and the data in Figure 5 show that the full AAV

capsids display dramatically higher levels of SYBR Gold staining than the empty capsids. In addition, the full capsid sample displayed a sixteen-fold increase in total particle count compared to the empty capsids. The full capsids also had a much higher percentage of particles (90% to 38.5%) that were stained with SYBR Gold. These data confirm that Aura GT can detect DNA from leaky, unstable AAV capsids and that this leakage is at least partially responsible for increased sub-visible aggregate formation.

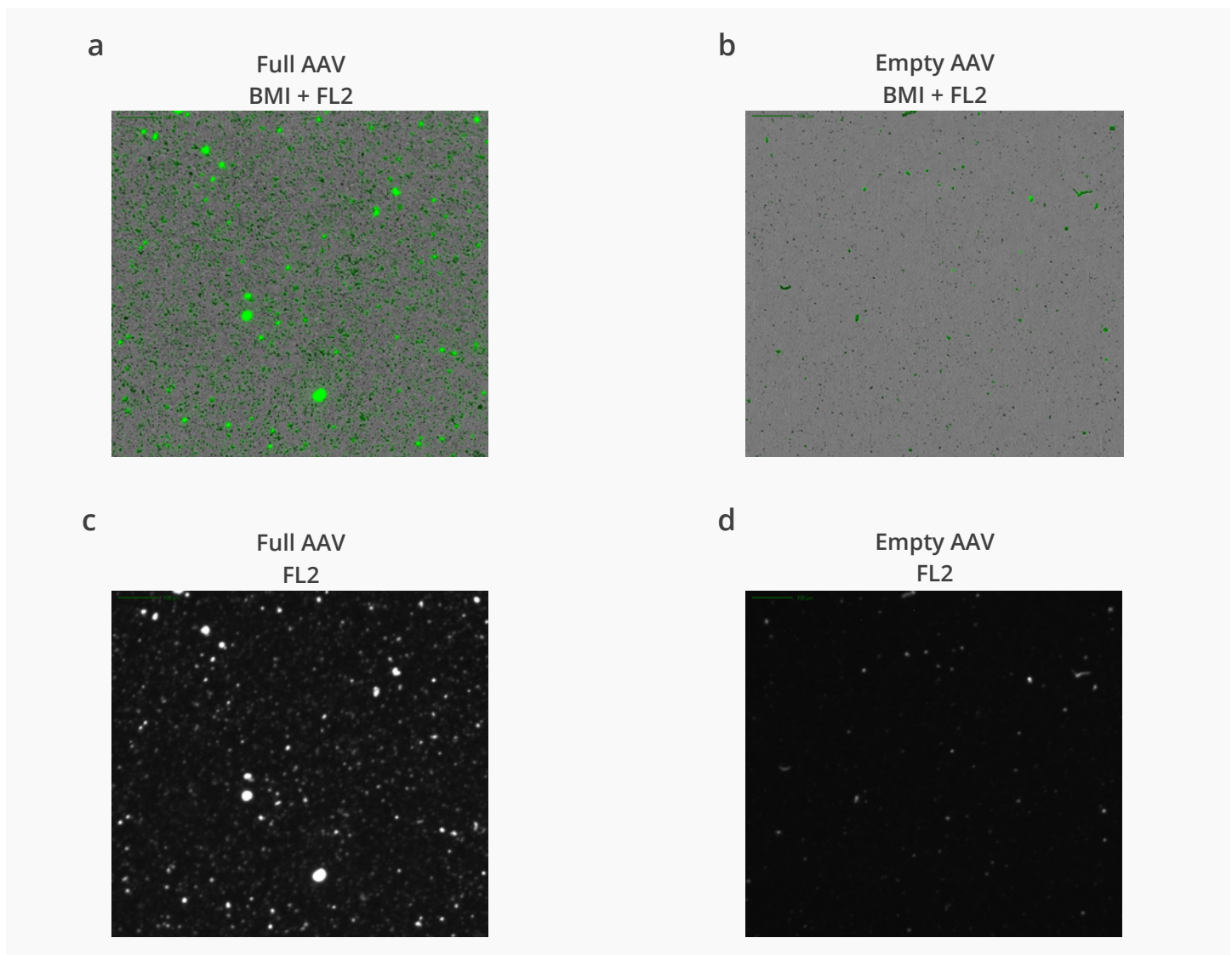


Figure 4: Aura GT can detect DNA leakage from an unstable AAV capsid. (a, c) Full and (b, d) empty AAV capsids well images. The full AAV capsids (left) showed a 16-fold increase in aggregation compared to the empty capsids (right) as well as a nearly 3x higher percentage of particles that were positive for SYBR Gold staining. Images are shown as a combined (a, b) Brightfield + SYBR Gold fluorescence and (c, d) SYBR Gold fluorescence only.

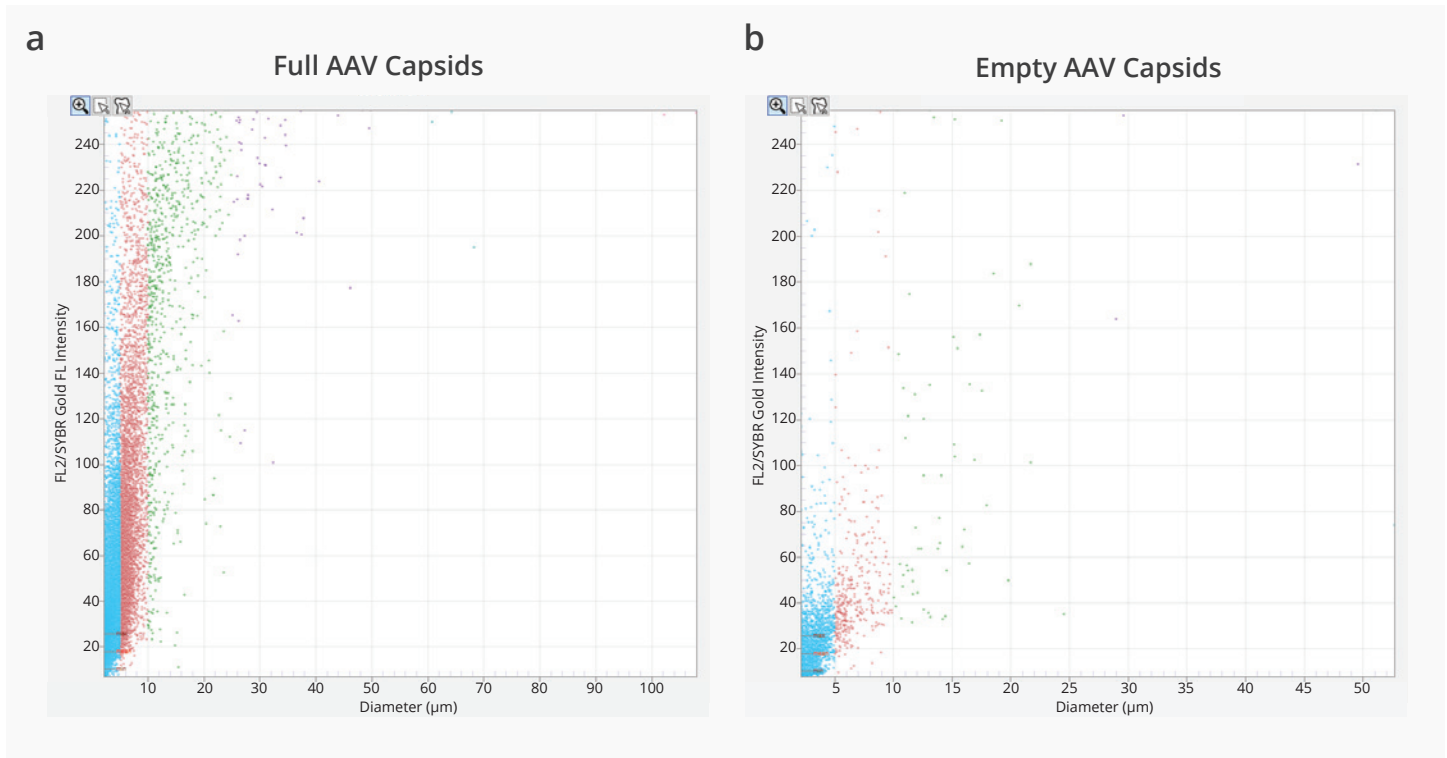



Figure 5: Scatterplot data for (a) full AAV capsids and (b) empty AAV capsids. The y-axis represents fluorescence intensity in the SYBR Gold channel, and the x-axis represents the equivalent circular diameter (ECD) for the individual particle. The full AAV capsid (left) had 16-fold as many particles and almost 3x stronger average fluorescence intensity than the empty capsid sample (right).

Conclusion

We have shown a significant difference in SYBR Gold staining between empty and full AAV capsids using Aura GT. Additional controls using amine conjugated beads with and without DNA confirm that the SYBR Gold binds to DNA and is detectable on Aura GT. The negative control data also show a lack of significant SYBR Gold fluorescence in BSA samples and no fluorescence in empty wells. The lack of SYBR Gold staining in BSA aggregates suggests that at least some of the weak signal seen in empty AAV capsids (Figure 4d) is likely from residual DNA, which is to be expected in any chromatographic separation. Taken together, the data confirm that Aura GT can detect the presence of DNA in subvisible aggregates using SYBR Gold staining. Most importantly, DNA leakage resulted in increasing subvisible particle formation. This information is key to AAV developers and formulators to establish the

most stable drug profile. In addition to characterizing the morphology of the AAV subvisible aggregates, Aura GT system identified the presence of both proteins and DNA using FMM. In this experiment, Aura GT characterized the particle morphology and the composition of aggregates in AAV drug products, allowing for precise optimization of the analytical and formulation development processes.

Aura GT provides a low-volume, high-throughput, and sensitive methodology for comprehensive AAV formulation development. It enables characterization of subvisible particles and their formation, and the impact of DNA leakage on sample stability. Aura GT's compatibility with USP 788 helps ensure the most important stability characteristic – subvisible particle concentration – can be monitored in AAV throughout the entire development process and through quality-control testing. 

References

1. Wang D, Tai PW, Gao G. (2019). Adeno-Associated Virus Vector as a Platform for Gene Therapy Delivery. *Nat Rev Drug Discov.* 18(5):358–78
2. Moussa EM, Panchal JP, Moorthy BS, Blum JS, Joubert MK, Narhi LO, Topp EM. (2016). Immunogenicity of Therapeutic Protein Aggregates. *J Pharm Sci.* 105(2):417–430
3. Bernaud J, Rossi A, Fis A, Gardette L, Aillot L, Büning H, Castelnovo M, Salvetti A, Faivre-Moskalenko C. (2018). Characterization of AAV Vector Particle Stability at the Single-Capsid Level. *J Biol Phys.* 44(2):181–94
4. Yin J, Chen R, Liu C. (2009). Nucleic Acid Induced Protein Aggregation and its Role in Biology and Pathology. *Front Biosci.* 14:5084–106

